PAPER

Fabrication of polyimide/graphene nanosheet composite fibers *via* microwave-assisted imidization strategy

Wei Jia,[a] Lingren Zhou,[a] Ming Jiang,[a] Jiang Du,[a] Mengying Zhang,[b] Enlin Han,[b] Hongqing Niu [ID] *[a] and Dezhen Wu*[a]

Here, a rapid and efficient strategy was introduced to prepare polyimide/graphene nanosheet (PI/GN) composite fibers by microwave-assisted imidization. The mechanical properties of the PI/GNs (1 wt%) fibers treated by microwave-assisted imidization were apparently improved with the tensile strength of 1.12 GPa at 350 °C, which was approximately 1.7 times as much as those treated with traditional thermal imidization. The PI/GNs (1 wt%) fibers heated by the microwave-assisted imidization method exhibited excellent thermal stabilities of up to 570.3 °C in nitrogen for a 5% weight loss, and a glass transition temperature above 339 °C. The results of the infrared spectrum and thermal properties indicated that the microwave-assisted treatment could promote the imidization degree of the PI/GN fibers prominently. Meanwhile, as a microwave absorber, graphene nanosheets (GNs) could also promote the imidization process by converting microwave energy into thermal energy. The microwave-polyimide/graphene nanosheet (MW-PI/GN) fibers possessed an optimum tensile strength of 1.38 GPa and modulus of 56.82 GPa at the GN content of 0.25 wt%. The 5% weight loss temperature in nitrogen ranged from 520.9 °C to 570.3 °C, and the glass transition temperature was increased from 305.7 °C to 339.1 °C with increasing the GN content.

1 Introduction

In recent years, polyimide (PI) fibers have been widely used in aerospace industries, microelectronic, and atomic energy industries owing to their excellent mechanical properties, high-temperature resistance, and superior chemical and irradiation resistance together with good dielectric properties.[1–4] With the deepening of industrialization upgrading, PI materials, as an "expert solution for solving material problems" have found an increasing demand in aerospace, safety protection, remote sensing mapping, photoelectric displays, and other fields. Further, improving the performance and yield to meet the needs of technological innovation and consumption growth in various industries is becoming an important direction for the study of PI materials.[5–8] The two-step method is the most widely used method to prepare PI materials, especially PI fibers, PI films, and other molding materials; however, this method also has its shortcomings: low utilization rate, large energy loss, and internal structural defects. Therefore, it is of great significance to optimize the preparation method of PI materials and to achieve the high-efficiency and energy-saving preparation of PI

materials while improving the performance.[9–11] However, some side effects, including oxidation and crosslinking, as well as insufficient utilization of energy should be considered during the high-temperature thermal imidization process.[12,13] It has been reported that microwave technology is an effective and green approach to heat materials, since it offers some advantages over conventional heating, such as non-contact and rapid heating from the interior of the material body.[14–20] Microwave-assisted heating to prepare polymer materials has unique advantages, including a faster reaction rate and higher conversion rate, and especially the phenomenon of promoting closed-loop polymerization. It provides a new idea for the imidization of PI materials and the preparation technology of PI fibers.[21–25] Li *et al.* synthesized the precursor polyamic acid (PAA) solution by the microwave-assisted heating method, and the yield was as high as 93% at 1.5 h.[26] Wang *et al.* used a microwave oven to cure the PI adhesive, and found that the curing effect from microwave heating was better than from the hot press and the electricity consumption cost was also greatly reduced.[27] Matsutani *et al.* used a temperature-controllable frequency conversion microwave device to achieve the imidization transformation of PAA films, and successfully prepared a complete imidized PI film.[28] Currently, there have been a few studies on the microwave-assisted heating method used to prepare PI materials, but there is a lack of discussion on the heating mechanism and influencing factors, while the changes in the internal structure and performance of PI materials during

[a]State Key Laboratory of Chemical Resource Engineering, College of Materials Science and Engineering, Beijing University of Chemical Technology, Beijing 100029, China. E-mail: wdz@mail.buct.edu.cn; niuhq@mail.buct.edu.cn; Fax: +86 10 6442 4654; +86 10 6442 1693; Tel: +86 10 6442 4654; +86 10 6442 1693

[b]Jiangsu Shino New Material and Technology Co., Ltd, Changzhou, 213000, China

the heating process have not been analyzed. This means the preparation of microwave-assisted heating PI materials lacks a sufficient theoretical basis and guidance. Consequently, use of the microwave-assisted heating method to prepare PI materials—especially the development of PI fibers, films and other materials with molding—is restricted.[29,30] In our previous work, a series of PI films were prepared *via* the microwave-assisted thermal imidization method. PI films obtained by this method possessed superior mechanical properties and better thermal properties than those obtained *via* thermal imidization, proving the microwave-assisted heating method's potential as a rapid and efficient way to prepare high-performance PI materials.[31] In addition, some microwave absorbers that interact with microwaves are used in the microwave-assisted process to produce more heat radiation, thereby promoting the closed-loop reaction. These microwave absorbers include carbon materials, such as carbon nanotube or graphene with sufficient dielectric loss.[32–34] Therefore, the addition of microwave absorbers can provide a novel way to fabricate PI materials, solving the problem of insufficient energy utilization. Most carbon materials, such as carbon nanotubes and graphene sheets, have a flowable π-electron cloud, which can allow interface polarization to take place under the action of a microwave field and generate a large amount of heat energy.[35–37] Therefore, GNs can be selected as a wave-absorbing filler, and the method of preparing polyimide/graphene nanosheets (PI/GNs) fibers *via* microwave-assisted imidization had the dual functions of filler reinforcement and wave-absorbing promotion of imidization. To the best of our knowledge, there has been no report regarding the application of microwave-assisted imidization and microwave absorbers in the preparation of PI fibers.

In this study, a series of PI/GNs fibers were prepared by the microwave-assisted imidization method to verify the effect of microwave-assisted heating and the ability of GNs as absorbers to convert microwave energy.

2 Experimental

2.1 Materials

The monomers *p*-phenylenediamine (PDA) and 4,4′-oxydianiline (ODA) were purchased from Changzhou Sunlight Pharmaceutical Co., Ltd. The monomer 3,3′,4,4′-biphenyltetracarboxylic dianhydride (BPDA) was purchased from Shijiazhuang Haili Chemical Company and purified by sublimation prior to use. The solvent dimethylacetamide (DMAc) was purchased from Beijing Chemicals Re-agent Factory and purified by distillation before use. Graphene nanosheets (GNs) were purchased from Jiangnan Graphene Research Institute. The deionized water used in the experiment was prepared using the Laboratory Water Purification System.

2.2 Preparation of the PI/CNs fibers

The PI/GNs fibers were prepared *via* the *in situ* polymerization and two-step method according to the following process. A mixture of GNs (1% wt), *p*-PDA, and ODA (molar ratio: 7/3) was dispersed in DMAc solvent by stirring in a dried atmosphere first, and then equimolar BPDA was added gradually to generate

the polyamic acid/graphene nanosheets (PAA/GNs) solution. The PAA/GNs precursor fibers were produced by extruding the viscous PAA/GNs solution through a spinneret, and then the PAA/GNs fibers were washed by deionized water to remove the residual solvent DMAc and then dried in an oven at 150 °C. The dried PAA/GNs fibers were heated in the oven at 200 °C, 250 °C, 300 °C, and 350 °C, respectively, to obtain the PI/GNs fibers, which were denoted as T-PI/GNs. Besides, the dried PAA/GNs fibers were placed in a microwave muffle furnace with a microwave magnetron and infrared temperature control system and heated following the same temperature process to obtain PI/GNs fibers by microwave-assisted imidization, and were denoted as MW-PI/GNs. Meanwhile, the pure PI fibers were prepared at 350 °C by microwave-assisted imidization, and were denoted as MW-PI. The PI/GNs fibers with different GNs content were prepared at 350 °C by microwave-assisted imidization, with the content of the GNs being 0.25, 0.5, 0.75, 1, and 2 wt%, denoting these as MW-PI/GNs-0.25G, MW-PI/GNs-0.5G, MW-PI/GNs-0.75G, MW-PI/GNs-1G, and MW-PI/GNs-2G, respectively. Scheme 1 illustrates the synthetic process for the BPDA/p-PDA/ODA copolymerization PI (co-PI). Fig. 1 illustrates the structure and preparation process of the PI/GNs fibers.

2.3 Characterization

Fourier transform infrared (FT-IR) spectra were obtained on a Nexus 670 instrument with the scanning wavenumber ranging from 4000 to 400 cm⁻¹ for an average of 16 scans. The samples were prepared by grinding the fibers with KBr in a mortar, and the measurements were conducted in ambient atmosphere. The imidization degree (ID) could be calculated using the equation:[11]

$$ID = \frac{(S1353/S1509)_i}{(S1353/S1509)_c} \times 100\% \qquad (1)$$

where S is the area of the absorption band, and subscript i and c represent the PI fibers with incomplete imidization and complete imidization, respectively.

The mechanical properties of the monofilaments were tested using a YG001A-1 instrument at an extension rate of 10 mm min⁻¹. At least 15 samples of each group were tested and the average value was achieved as a result.

Two-dimensional wide-angle X-ray diffraction (2D WAXD) was performed on a Bruker D8 Discover diffractometer equipped with
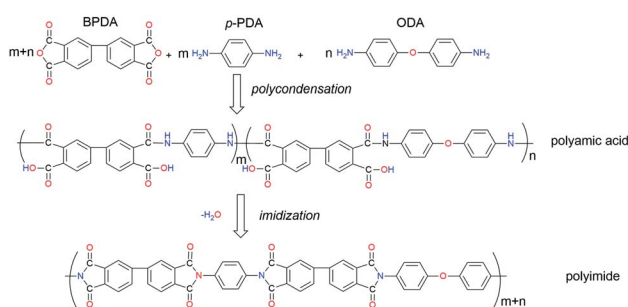
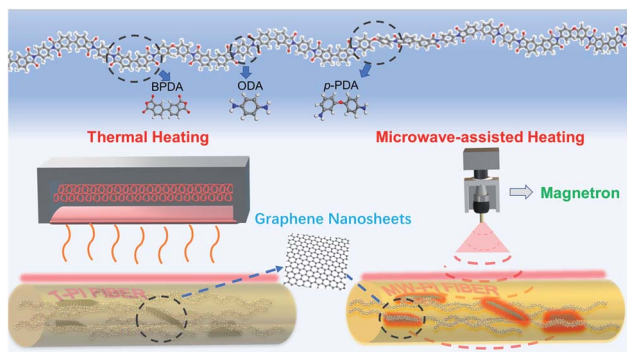**Scheme 1** Synthetic process of BPDA/p-PDA/ODA co-PI.

Fig. 1 Structure and preparation process of PI/GNs fibers.

GADDS as a 2D detector. X-ray diffraction measurements were taken in transmission mode at room temperature. The instrument employed Cu Kα radiation ($\lambda = 0.154$ nm) and operated at 40 kV and 40 mA. A bundle of closely packed parallel fibers were fixed on the specimen holder by double-sided tape, and the point-focused X-ray beam was aligned perpendicular to the fiber axis direction. The crystal interlayer d-spacing was calculated using Bragg's reflection equation:

$$n\lambda = 2d \sin \theta \qquad (2)$$

In addition, the degree of molecular orientation could be calculated by integrating the corresponding intensities of the azimuthal scans along the isolated and preferred crystal planes. The degree of molecular orientation of the fibers was calculated based on the Herman's equation:[38]

$$f = \left(\langle 3\cos^2\varphi - 1 \rangle \right)/2 \qquad (3)$$

where f is the degree of molecular orientation along the fiber axis direction and φ represents the angle between the fiber axis and c-axis crystal unit cell. The numerical values of the mean square cosines in the equation above were determined by corrected intensity distribution $I(\varphi)$ diffracted from the crystalline plane by Gaussian fitting following the equation:[39]

$$\langle \cos^2\varphi \rangle = \frac{\int_0^{\pi/2} I(\varphi)\sin\varphi\cos^2\varphi \, d\varphi}{\int_0^{\pi/2} I(\varphi)\sin\varphi \, d\varphi} \qquad (4)$$

Dynamic mechanical analysis (DMA) was performed on a DMA Q800 system with a load frequency of 1 Hz and heating rate of 5 °C min^{-1} at temperatures ranging from 50 °C to 450 °C.

Thermogravimetric analysis (TGA) measurements were carried out on a TGA Q50 system with a heating rate of 10 °C min^{-1} from 50 °C to 800 °C under nitrogen.

The morphologies of the fractured surfaces were captured on a Hitachi S-4700 system.

3 Results and discussion

3.1 Chemical structure

Fig. 2 shows the FT-IR spectra of the PI/GNs fibers prepared at different temperatures. All the PI fibers displayed four characteristic absorption peaks at approximately 1778, 1715, 732, and 1353 cm^{-1}, which were attributed to the C=O asymmetrical stretching, symmetrical stretching and bending, and C–N stretching of the cyclic imide, respectively. The absorption band at 1850 cm^{-1}, which was assigned to terminal anhydride generated by the degradation of PAA chains, could be observed in the spectra of the T-PI/GNs-200 and T-PI/GNs-250 fibers. Nevertheless, the absorption bands at 1850 cm^{-1} for the MW-PI/GNs-200 fibers became weaker and MW-PI/GNs-250 fibers were absent, indicating that microwave-assisted imidization treatment could inhibit the dissociation of PAA molecular chains effectively. Furthermore, the intensities of C–N (1353 cm^{-1}) of the MW-PI/GNs fibers were always stronger than those of the T-PI/GNs fibers, implying that microwave-assisted treatment could promote the conversion to cycloimide rings. Table 1 lists the IDs of the MW-PI/GNs and T-PI/GNs fibers with different temperatures. The ID of MW-PI/GNs-350 was set as 100%. It is obvious that the IDs of the MW-PI/GNs fibers were higher than those of the T-PI/GNs fibers.

The ID values of the T-PI/GNs-350 and MW-PI/GNs-300 fibers were calculated as 85.8% and 93.2%, indicating that the microwave-assisted heating method could accelerate the imidization process and reduce the cyclization temperature significantly. Table 2 lists the variation of the IDs with the different GNs content. The IDs increased gradually for the MW-PI/GNs fibers with a higher GN content, indicating that the GNs could promote the imidization degree of the PI fibers by
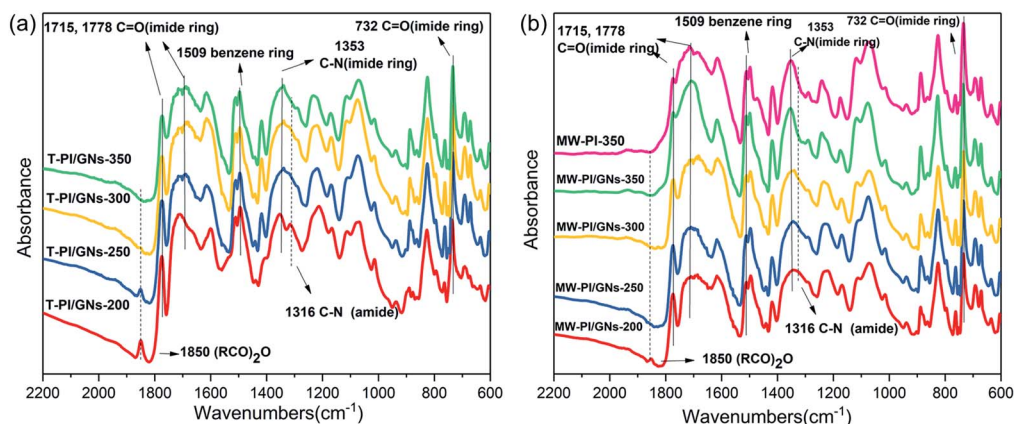

Fig. 2 FT-IR spectra of the PI/GNs fibers ((a) T-PI/GNs; (b) MW–PI/GNs).

Table 1   ID values of the PI/GNs fibers at different temperatures

T/°C	ID (T-PI/GNs, %)	ID (MW-PI/GNs, %)
200	24.7	41.3
250	31.1	68.9
300	54.9	93.2
350	85.8	100.0

Table 2   ID values of the MW-PI/GNs fibers with different GNs content

Sample	ID (%)
MW-PI/GNs-0G	89.2
MW-PI/GNs-0.25G	92.9
MW-PI/GNs-0.5G	96.5
MW-PI/GNs-0.75G	96.8
MW-PI/GNs-1G	100.0
MW-PI/GNs-2G	97.1

converting microwave energy into thermal energy. At the same time, GNs are good microwave absorbing carriers and are dispersed in the PI fiber matrix, thus promoting synchronous heating from inside to outside of the fiber and avoiding the occurrence of an "imination gradient". However, too high a GN content caused local overheating, thus the imidization degree of MW-PI/GNs-2G fibers dropped to 97.1%.

3.2   Mechanical properties

The tensile strength, initial modulus, and elongation at break of the MW-PI/GNs and T-PI/GNs fibers with different treatment temperatures are listed in Table 3. The mechanical properties of both the T-PI/GNs and MW-PI/GNs fibers were improved with increasing the temperature, reaching the optimum at 350 °C.

Obviously, the tensile strength and initial modulus of the MW-PI/GNs fibers were higher than those of the T-PI/GNs fibers, proving the promotion of microwave irradiation upon the imidization process. The MW-PI/GNs-350 fibers possessed the optimal modulus of 53.53 GP and tensile strength of 1122.56 MPa. Moreover, the tensile strength of the MW-PI/GNs-

Table 3   Mechanical properties of the T-PI/GNs and MW-PI/GNs fibers

Sample	Tensile strength (MPa)	Elongation (%)	Initial modulus (GPa)
T-PI/GNs-200	147.13	1.45	21.47
MW-PI/GNs-200	348.05	6.20	27.18
T-PI/GNs-250	227.28	3.30	12.63
MW-PI/GNs-250	708.19	4.35	32.12
T-PI/GNs-300	447.05	7.11	19.70
MW-PI/GNs-300	964.35	7.00	37.88
T-PI/GNs-350	656.43	8.80	26.35
MW-PI/GNs-350	1122.56	4.95	53.53
MW-PI-350	1053.00	4.91	46.93

Table 4   Mechanical properties of MW-PI/GNs fibers with different GNs content

Sample	Tensile strength (MPa)	Elongation (%)	Initial modulus (GPa)
MW-PI/GNs-0.25G	1386.0	3.24	56.82
MW-PI/GNs-0.5G	1323.8	4.54	54.01
MW-PI/GNs-0.75G	1160.2	4.67	53.52
MW-PI/GNs-1G	1122.6	4.95	53.53
MW-PI/GNs-2G	838.9	2.10	44.46

350 fibers was 6.6% higher than that of the MW-PI-350 fibers due to the incorporation of GNs, thus confirming the positive effect of GNs as microwave absorbers upon the imidization process of the PI fibers. In addition, the GNs were inclined to lay flat and orient along the direction of the molecular chains at high drawing ratios during the wet-spinning process, thus enhancing the mechanical properties of the MW-PI/GNs fibers. Given the excellent fracture strength and Young's modulus of the GNs, it could be expected that the mechanical properties of PI/GNs fibers would be enhanced by the uniform dispersion of GNs in the polymer matrix. Table 4 lists the variation of the mechanical properties with the GNs content. The tensile strength ranged from 838.9 MPa to 1386 MPa, initial modulus ranged from 44.46 GPa to 56.82 GPa, and the elongation at break ranged from 2.10% to 4.95%, respectively. The tensile strength and modulus reached peak values of 1386 MPa and 56.82 GPa at 0.25 wt% GNs loading, which were 31.6% and 21.1% higher than those of MW-PI fibers, indicating that the addition of GNs significantly improved the mechanical properties of the fibers. This promotion arises from two aspects. On the one hand, GNs dispersed in the PI fiber matrix are good microwave absorbing carriers, which achieves the simultaneous heating inside and outside of the fiber with the help of microwave and avoids the occurrence of an "imination gradient". On the other hand, in the process of preparing PI primary fibers by wet-spinning, the spinning solution is highly stretched and fixed in the coagulation bath when it is sprayed through the spinneret. The CNs alignment can be improved by drawing out the processing, and most of the CNs can then be well aligned along the drawing direction, which, together with the help of its high specific surface area and strength, improves the mechanical properties of the MW-PI/GNs fibers. However, due to the GNs not having surface modification, it is easy to for them to agglomerate when adding more GNs, which destroys the structure between the molecular chains and leads to a decrease in the mechanical properties. Therefore, the tensile strength and initial modulus of MW-PI/GNs-0.25G to MW-PI/GNs-1G gradually decreased, and the elongation at break increased. In particular, the continuous increase in loading of GNs to 2 wt% caused an apparent decrease in the mechanical properties.

3.3   Aggregation structure

The aggregation structure of PI fibers, including the molecular packing and orientation, plays an important role in their final

Table 5 The *d*-spacing and orientation degree of the PI fibers

Sample	*d*-spacing (nm)	Orientation degree (%)
MW-PI-350	0.796	85.1
T-PI/GNs-350	0.776	78.1
MW-PI/GNs-350	0.790	89.2

Fig. 4 2D WAXD patterns and WAXD intensity profiles of the MW-PI/GNs fibers with different GNs content (A: 0.25G; B: 0.5G; C: 0.75G; D: 1G; E: 2G; F: meridional directions; G: equatorial directions).

performance. There was no evidence of diffraction in the quadrants, implying the absence of a well-defined 3D crystalline structure of the PI fibers prepared in the present work. Fig. 3 shows the 2D WAXD patterns of the PI fibers. In the meridian direction, all the fibers exhibited clear diffraction streaks, presenting a high orientation in the fiber axial direction. Two Bragg diffraction streaks at $11.4°$ ($d = 0.776$ nm) and $17.1°$ ($d = 0.518$ nm) could be observed, which were assigned to be the (002) and (003) planes, respectively. In comparison with the T-PI/GNs-350 fibers, the MW-PI/GNs-350 and MW-PI-350 fibers exhibited narrower and clearer diffraction streaks in the meridional direction, indicating a higher orientation degree along the fiber axial direction. At the same time, the microwave-assisted heating method made the fibers more homogeneous in structure and the molecular packing more compact. Therefore, the molecules were adequately aligned along the axis, resulting in a larger orientation factor. The (002) *d*-spacing of the MW-PI/GNs-350 fibers was calculated as 0.790 nm according to Bragg's Law, which was 0.014 nm higher than that of the T-PI/GNs-350 ones, revealing that microwave-assisted treatment could improve the ordered arrangement of the PI macromolecule chains (Table 5). Compared with the MW-PI-350 fibers, the MW-PI/GNs-350 fibers exhibited broader diffraction streaks in the meridional direction and more diffuse halos in the equatorial direction, indicating an increase in the crystallinity, which was due to the incorporated GNs being able to promote an adequate movement of the inner and outer molecular chains by converting microwaves into heat energy and promoting a closer accumulation of molecular chains. Under the action of
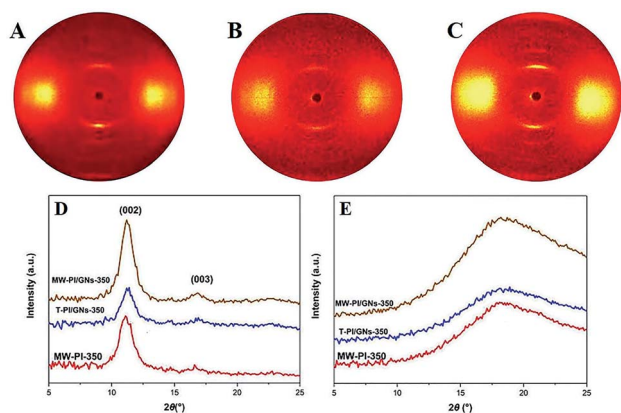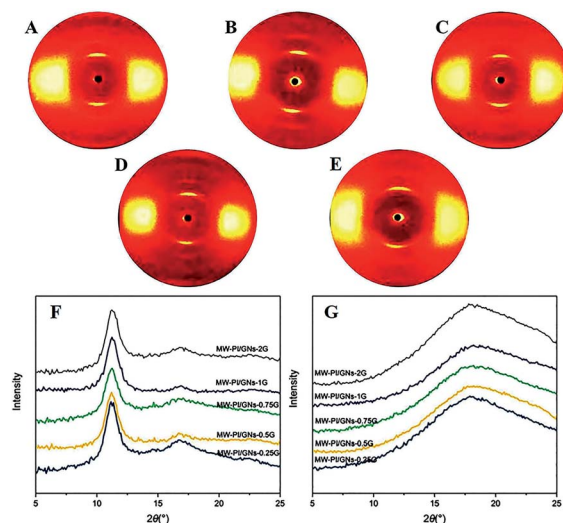
heat, the molecular chains could adequately move and stretch, which helps promote the regular and orderly arrangement of the molecular chain structure, thereby increasing the degree of orientation.

Fig. 4 presents the WAXD diffraction spectra and intensity profiles of the MW-PI/GNs fibers with different GNs content in the meridian and equatorial directions. In the equator direction, the diffraction pattern varied with the different GNs content, indicating that the incorporation of GNs had a tremendous effect on the microstructure of the fibers. In the meridian direction, two diffraction peaks at $2\theta = 11.25°$ ($d = 0.786$ nm) and $16.94°$ ($d = 0.523$ nm) could be observed for the MW-PI/GNs fibers, which were, respectively, set to be the (002) and (003) planes according to our previous work. Additionally, the degree of molecular orientation of the (002) plane of the MW-PI/GNs fibers was calculated, as listed in Table 6. All the fibers exhibited a high degree of orientation over 80%, which implied the presence of a highly oriented structure along the fiber axial direction. The molecular chains were arranged axially, and the orientation factor of the MW-PI/GNs fibers ranged from 83.4% to 92.7%. Such variety is consistent with the mechanical properties. With the further increase in the GNs content, the agglomeration phenomenon gradually became obvious, and the orderly arrangement of the molecular chains was destroyed to a certain extent, resulting in a decrease in the orientation factor.

3.4 Thermal properties

The 5% weight loss temperature (T_{d5}) and T_g of the PI/GNs-350 fibers are shown in Fig. 5. The data demonstrate the excellent thermal stability of the MW-PI/GNs-350 fibers with a T_{d5} of up to 570.3 °C, which was highly superior to that of the T-PI/GNs-350 fibers (512.8 °C), indicating that the microwave heating had a positive effect on improving the thermal stabilities of the PI

Fig. 3 2D WAXD patterns ((A) MW-PI-350, (B) T-PI/GNs-350, (C) MW-PI/GNs-350) and WAXD intensity profiles of the PI fibers ((D) meridional direction; (E) equatorial direction).

Table 6 The *d*-spacing (nm) and orientation degree of the MW-PI/GNs fibers

Sample	*d*-Spacing (nm)	Orientation degree (%)
MW-PI/GNs-0.25G	0.799	92.7
MW-PI/GNs-0.5G	0.795	90.3
MW-PI/GNs-0.75G	0.789	90.7
MW-PI/GNs-1G	0.790	89.2
MW-PI/GNs-2G	0.789	83.4

Fig. 6 The TGA curves and DMA curves of MW-PI/GNs fibers with different GNs content.
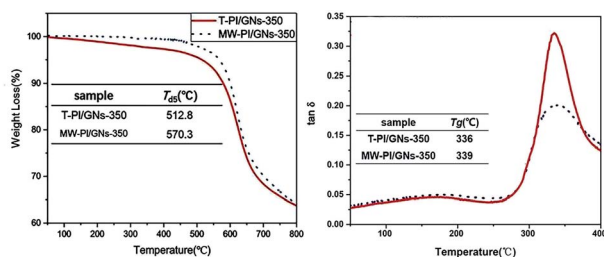
Fig. 5 The TGA curves and DMA curves of the PI/GNs fibers.

fibers. The T_g of the MW-PI/GNs-350 fibers was also higher than that of the T-PI/GNs-350 fibers, which is suggested to be caused by its higher degree of molecular orientation, thus inhibiting the segments mobility. The tanδ value of the MW-PI-350 fibers was lower than that of the T-PI/GNs fibers, and this phenomenon can be explained by the following contributions. On the one hand, the degree of imidization was improved by microwave-assisted heating, while on the other hand, the perfect molecular chain structure improved the storage modulus. As shown in Fig. 6, the thermal stability of the MW-PI/GNs fibers increased first and then decreased with increasing the GNs content. The T_{d5} of MW-PI/GNs-1G reached a maximum of 570.3 °C, while MW-PI/GNs-2G dropped to 529.7 °C. This phenomenon may be due to the poor dispersibility of the agglomerated GNs particles, which not only destroys the close arrangement of molecular chains, but also causes partial overheating during absorbing heating, resulting in the degree of imidization and thermal stability decreasing. The addition of GNs improved the thermal stability of the MW-PI/GNs fibers, which may arise from two aspects: on the one hand, the addition of GNs improved the ordering of the PI fibers and played a part in the crosslinking. This promoted the close arrangement of molecular chains, so that the imide ring could not be easily attacked by free radicals under high-temperature conditions; while on the other hand, the absorbing effect of GNs converted microwave energy into heat energy, promoted the cyclization of molecular chains, and improved the thermal stability of the PI fibers. This phenomenon could be further analyzed by the dynamic thermomechanical performance. The DMA curves of the PI fibers were evaluated at a heating rate of 5 °C min^{-1} from 50 °C to 450 °C in a nitrogen atmosphere, as shown in Fig. 6. The peaks identified in the curves reflect the α relaxation of the molecular chains. The temperature corresponding to the α relaxation is identified as the glass transition
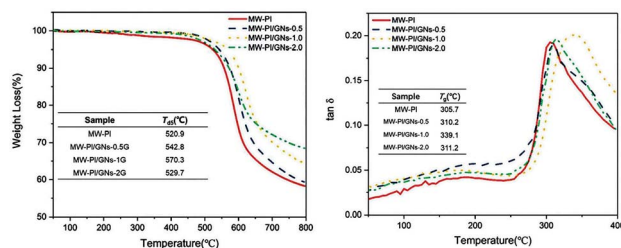
temperature (T_g) of the fibers. Their T_g values were 305.7 °C, 310.2 °C, 339.1 °C, and 311.2 °C, which corresponded to GNs contents of 0, 0.5, 1.0, and 2.0, respectively. In addition, the T_{d5} of the MW-PI/GNs-350 fibers was also significantly higher than that of the MW-PI-350 fibers, indicating that the conversion of microwave energy into heat energy by GNs improved the degree of imidization. Moreover, GNs have excellent temperature resistance, so the thermal stability of the composite fibers was improved by combining the two factors. Also, the GNs hinder the segmental motion of polymer chains to some extent, resulting in an increase in T_g. Therefore, it could be observed that the T_g of the MW-PI/GNs-350 fibers (339 °C) was higher than that of the MW-PI-350 fibers (305.7 °C).

3.5 Morphologies

SEM was used to characterize the morphology of the composite fibers. The fracture morphologies of the PI fibers are shown in Fig. 7. The fracture morphologies of the MW-PI/GNs-350 fibers and MW-PI-350 fibers were more dense, while the T-PI/GNs-350 fibers formed a relatively neat fracture, resulting from the decreased mechanical properties. Compared with the MW-PI-350 fibers, a certain degree of microfibrils appeared on the external skin of the MW-PI/GNs-350 fibers, revealing that the MW-PI/GNs-350 fibers possessed a higher oriented molecular chain structure with the supplement of the GNs, which was consistent with the result of mechanical properties. The results show that microwave-assisted imidization can significantly improve the structure and properties of the fibers without causing a rapid evaporation of the residual solvents and water to produce pores in the fibers.

4 Conclusions

In summary, PI/GNs fibers were successfully prepared *via* a thermal imidization method and microwave-assisted
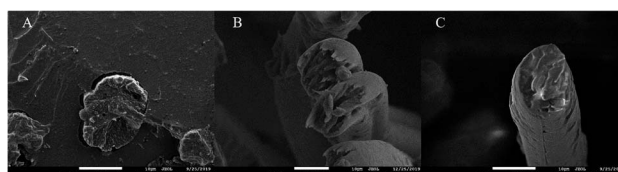

Fig. 7 The fracture morphologies of the PI fibers. (A) T-PI/GNs-350; (B) MW-PI/GNs-350; (C) MW-PI-350.

imidization method at 200–350 °C, respectively. The results from FT-IR and 2D WAXD analyses revealed that microwave irradiation had a positive effect on reducing the imidization temperature, and improving the imidization degree, as well as the macromolecular order degree, thus enhancing the mechanical properties and thermal stability of the PI fibers. The tensile strength of the MW-PI/GNs-350 fibers was 1122.56 MPa, which was about 1.7 times that of the T-PI/GNs-350 fibers, and its thermal stability was as high as 570.3 °C of T_{d5} in nitrogen. As confirmed by the 2D WAXD data results, the MW-PI/GNs fiber chains preferred an ordered molecular alignment, but due to the agglomeration phenomenon, the molecular orientation decreased gradually with the increased GNs content. The GNs played an important role in absorbing the microwave energy, hence the mechanical properties and thermal stabilities of the MW-PI/GNs-350 fibers were higher than those of the MW-PI-350 fibers. In addition, the incorporation of GNs restricted the macromolecular segments movement, thus enhancing the T_g of the MW-PI/GNs-350 fibers prominently. In a nutshell, the combination of the microwave-assisted imidization method and microwave absorbers opens up a broader avenue for the manufacturing and processing of PI fibers.

Conflicts of interest

There are no conflicts to declare.

Acknowledgements

Notes and references

1 M. Hasegawa and K. Horie, *Prog. Polym. Sci.*, 2001, **26**, 259–335.
2 J. Dong, C. Yin, Y. Zhang and Q. zhang, *J. Polym. Sci.*, 2014, **52**, 450–459.
3 D. J. Liaw, K. L. Wang, Y. C. Huang, K. R. Lee, J. Y. Lai and C. S. Ha, *Prog. Polym. Sci.*, 2012, **37**, 907–974.
4 G. A. Bernier and D. E. Kline, *J. Appl. Polym. Sci.*, 1968, **12**, 593–604.
5 M. Katz and R. J. Theis, *IEEE Electron. Ind. Mag.*, 1997, **13**, 24–30.
6 S. Duo, L. I. Mei-Shuan and Y. C. Zhou, *Trans. Nonferrous Metals Soc. China*, 2006, **16**, 661–664.
7 W. Jang, S. Sundar, S. Choi, Y. Shul and H. Han, *J. Mem. Sci.*, 2006, **280**, 321–329.
8 M. T. Bogert and R. R. Renshaw, *J. Am. Chem. Soc.*, 1908, **30**, 1135–1144.
9 H. Niu, M. Huang, S. Qi, E. Han, G. Tian, X. Wang and D. Wu, *Polymer*, 2013, **54**, 1700–1708.
10 K. Vanherck, G. Koeckelberghs and I. F. J. Vankelecom, *Prog. Polym. Sci.*, 2013, **38**, 874–896.
11 Y. Zhai, Q. Yang, R. Zhu and Y. Gu, *J. Mater. Sci.*, 2008, **43**, 338–344.
12 J. Tierney, B. Wathey and J. Westman, *Tetra*, 2001, **57**, 9225–9283.
13 E. James, *Phys. Today*, 1985, **38**, 60–67.
14 R. Gedye, F. Smith, K. Westaway, H. Ail, L. Baldisera, L. Laberge and J. Rousell, *Tetrahedron Lett.*, 1986, **27**, 279–282.
15 C. O. Kappe and D. Dallinger, *Mol. Diversity*, 2009, **13**, 71–193.
16 J. A. Menéndez, A. Arenillas, B. Fidalgo, Y. Fernández, L. Zubizarreta, E. G. Calvo and J. M. Bermúdez, *Fuel Process. Technol.*, 2010, **91**, 1–8.
17 C. Gabriel, S. Gabriel, E. H. Grant, *et al.*, *Chem. Soc. Rev.*, 1998, **27**, 213–223.
18 E. Vázquez and M. Prato, *ACS Nano*, 2009, **3**, 3819–3824.
19 C. Ebner, T. Bodner, F. Stelzer and F. Wiesbrock, *Macromol. Rapid. Comm.*, 2011, **32**, 254–288.
20 M. Bardts, N. Gonsior and H. Ritter, *Macromol. Chem. Phys.*, 2008, **209**, 25–31.
21 Y. Li, L. Cheng and J. Zhou, *Int. J. Adv. Des. Manuf. Technol.*, 2018, **5**, 1–11.
22 V. Tanrattanakul and D. Jaroendee, *J. Appl. Polym. Sci.*, 2006, **102**, 1059–1070.
23 B. T. Ginn and O. Steinbock, *Langm*, 2003, **19**, 8117–8118.
24 T. L. White, F. L. Paulauskas, and T. S. Bigelow, *US Pat.*, 7824495B1, 2017.
25 Y. Imai, H. Nmoto and M. A. Kakimoto, *J. Polym. Sci., Part A: Polym. Chem.*, 1996, **34**, 701–704.
26 Q. Li, Z. Xu and C. Yi, *J. Appl. Polym. Sci.*, 2008, **107**, 797–802.
27 K. Wang, X. Yuan and M. Zhan, *Int. J. Adhes. Adhes.*, 2017, **74**, 28–34.
28 H. Matsutani, T. Hattori, M. Ohe, *et al.*, *J. Photopolym. Sci. Technol.*, 2005, **18**, 327–332.
29 B. Govindaraj and M. Sarojadevi, *Polym. Compos.*, 2016, **37**, 2417–2424.
30 V. S. Kishanprasad and P. H. Gedam, *J. Appl. Polym. Sci.*, 1993, **50**, 419–429.
31 L. Lin, P. Ye, C. Cao, Q. Jin, *et al.*, *J. Mater. Chem. A*, 2015, **3**, 10205–10208.
32 L. Zhou, Y. Li, Z. Wang, M. Zhang, X. Wang, H. Niu and D. Wu, *RSC Adv.*, 2019, **9**, 7314–7320.
33 M. Park, B. Ramaraj and K. Yoon, *Appl. Surf. Sci.*, 2012, **258**, 8656–8661.
34 J. Long, M. Fang and G. Chen, *J. Mater. Chem.*, 2011, **21**, 10421–10425.
35 N. D. Kim, A. Metzger, V. Hejazi, *et al.*, *ACS Appl. Mater. Interfaces*, 2016, **8**, 12985–12991.
36 M. Odom, C. Sweeney, D. Parviz, *et al.*, *Carbon*, 2017, **120**, 447–453.
37 J. Dong, C. Yin, X. Zhao, Y. Li and Q. Zhang, *Polymer*, 2013, **54**, 6415–6424.
38 M. Zhang, H. Niu, Z. Lin, S. Qi, J. Chang, Q. Ge and D. Wu, *Macromol. Mater. Eng.*, 2015, **300**, 1096–1107.
39 M. Hasegawa, N. Sensui, Y. Shindo, *et al.*, *J. Polym. Sci., Polym. Phys. Ed.*, 1999, **37**, 2499–2511.